NANO · MICRO small
www.small-journal.com

# Controllable Fabrication of Inhomogeneous Microcapsules for Triggered Release by Osmotic Pressure

*Weixia Zhang, Liangliang Qu, Hao Pei, Zhao Qin, Jonathan Didier, Zhengwei Wu, Frank Bobe, Donald E. Ingber, and David A. Weitz**

**Inhomogeneous microcapsules that can encapsulate various cargo for controlled release triggered by osmotic shock are designed and reported. The microcapsules are fabricated using a microfluidic approach and the inhomogeneity of shell thickness in the microcapsules can be controlled by tuning the flow rate ratio of the middle phase to the inner phase. This study demonstrates the swelling of these inhomogeneous microcapsules begins at the thinnest part of shell and eventually leads to rupture at the weak spot with a low osmotic pressure. Systematic studies indicate the rupture fraction of these microcapsules increases with increasing inhomogeneity, while the rupture osmotic pressure decreases linearly with increasing inhomogeneity. The inhomogeneous microcapsules are demonstrated to be impermeable to small probe molecules, which enables long-term storage. Thus, these microcapsules can be used for long-term storage of enzymes, which can be controllably released through osmotic shock without impairing their biological activity. The study provides a new approach to design effective carriers to encapsulate biomolecules and release them on-demand upon applying osmotic shock.**

Dr. W. Zhang, Dr. L. Qu, Dr. H. Pei, Dr. J. Didier, Z. Wu, Prof. D. E. Ingber, Prof. D. A. Weitz
John A. Paulson School of Engineering and Applied Sciences
Harvard University
Cambridge, MA 02138, USA
E-mail: weitz@seas.harvard.edu

Dr. W. Zhang, Dr. L. Qu, Dr. H. Pei, Dr. J. Didier, Z. Wu, Dr. F. Bobe, Prof. D. E. Ingber, Prof. D. A. Weitz
Wyss Institute for Biologically Inspired Engineering
at Harvard University
Boston, MA 02115, USA

Dr. Z. Qin
Department of Civil and Environmental Engineering
Syracuse University
Syracuse, NY 13244, USA

Z. Wu
Department of Biomedical Engineering and Biotechnology
University of Massachusetts Lowell
Lowell, MA 01854, USA

Prof. D. E. Ingber
Vascular Biology Program and Department of Surgery
Boston Children's Hospital and Harvard Medical School
Boston, MA 02115, USA

The ORCID identification number(s) for the author(s) of this article can be found under https://doi.org/10.1002/smll.201903087.

**DOI: 10.1002/smll.201903087**

Developing carriers of active ingredients with triggered-release properties is an important challenge in the field of controlled release.[1] Stimuli-responsive microcapsules, as effective carriers, have been widely used to encapsulate various valuable cargoes, including nanomaterials, essential oils, colorings, flavorings, bioactive molecules, and living cells, for long-term storage without any deterioration.[2–7] Equally important, the encapsulated cargoes should be released to perform their functionalities when microcapsules respond to external stimuli. For instance, encapsulated drugs need to be released for therapeutic treatment. A variety of external stimuli, including temperature, pH, light, magnetic field, or stress, can be utilized to trigger the release of encapsulated contents via chemical or physical changes to the shell materials.[8–17] Chemical changes can be initiated by a trigger that causes cross-link cleavage or depolymerization of the shell materials.[9,17–20] While this technique allows active release of cargo, its utility is limited because it requires microcapsules with multiple functionalities in the shell materials, which usually requires complicated synthesis or fabrication. A simple strategy to circumvent this limitation is to trigger the release through mechanical cracking of the shell wall when the shell material undergoes a physical change, such as pressure-induced failure, shell wall melting or a change in porosity.[21,22] Several triggers can be used to induce physical changes, including mechanical stress or osmotic pressure.[23,24] Osmotic pressure is an effective trigger to rupture the microcapsule shell for burst release of the cargoes by simply adding water to the microcapsule system. The osmotic pressure is usually generated by introducing an osmotic agent to the core. Due to the osmotic pressure difference across the shell, water diffuses into the core, resulting in swelling of microcapsule; the microcapsule bursts when the shell cannot withstand the deformation and rapidly releases the cargo.

Microcapsules with uniform shell thickness swell isotropically upon introduction of a small internal osmotic pressure, and they ultimately reach isotonic conditions when the osmotic pressure difference across the shell becomes negligible. To achieve burst release, the internal pressure of the microcapsules has to exceed the failure strength of the shell material before the microcapsules reach isotonic conditions. Therefore, it can

 

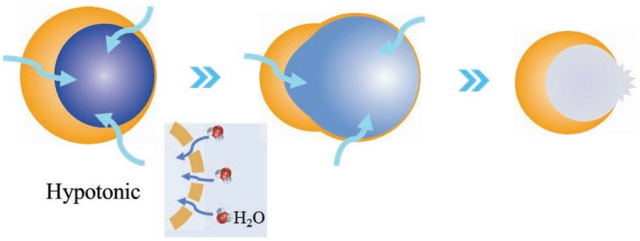


**Figure 1.** Schematic illustration of asymmetric swelling of a microcapsule with inhomogeneous shell thickness under hypotonic condition. The microcapsule ultimately ruptures at the thinnest part of shell.

require coencapsulation of a large concentration of osmotic agents to trigger the cargo release for microcapsules with homogeneous shell thickness, which also needs high osmotic pressure in the outer solution to balance the internal and external pressures before the release is induced. As a result, undesirable additives may have to be introduced into both the internal core and the outer solution; this not only makes the encapsulation system less efficient and less economic, but may lead to problems for some specific applications. For example, in biomedical applications, a solution with high osmotic pressure can cause tissue injury or induce blood clot formation.[25,26] Thus, if it were possible to create microcapsules that can be triggered to release their contents based on pressure differentials without requiring very high solute concentrations in the solution, it could open up entirely new applications in controlled release.

In this paper, we use a microfluidic technique to fabricate stimuli-responsive microcapsules with inhomogeneous shell thickness, which can be triggered to release the encapsulated cargo at a low rupture osmotic pressure. The inhomogeneity in shell thickness can be tuned by changing the ratio of the flow rate of the middle phase, $Q_m$, to the inner phase, $Q_i$. Interestingly, unlike isotropic swelling of microcapsules with a uniform shell, the swelling of inhomogeneous microcapsules begins at the thinnest part of shell and eventually leads to rupture at the weak spot, as shown in **Figure 1**. We find that the required rupture osmotic pressure to make inhomogeneous microcapsules rupture is much lower than that for microcapsules with uniform shell thickness. In addition, we systematically study the relationship between shell inhomogeneity and the rupture behavior of microcapsules, and observe an empirical linear relationship between them. Remarkably, the microcapsule shell is impermeable to small probe dye molecules, which is very important for long-term storage. Finally, we demonstrate our approach can encapsulate a model enzyme for triggered release by osmotic pressure without impairing their biological activity.

We use a glass capillary microfluidic device to fabricate microcapsules with inhomogeneous shell thickness based on water-in-oil-in-water (W/O/W) double emulsion templates.[27] The glass capillary device consists of two tapered cylindrical glass capillaries with different tip sizes that are coaxially aligned within a square capillary, as shown schematically in **Figure 2**a. We use the capillary with a smaller tip to inject the inner phase consisting of sucrose in 3 wt% poly(vinyl alcohol) (PVA) aqueous solution. Sucrose is used as an agent to increase the osmotic pressure of the inner phase. Photocurable monomers in dichloromethane are used as the middle oil phase and are injected through the interstices between the square capillary and the injection capillary. The monomers used are poly(ethylene glycol) divinyl ether and trimethylolpropane tris(3-mercaptopropionate). Under UV exposure, they rapidly react with each other, in what is known as the thiol-ene reaction. The continuous phase, which is $CaCl_2$ in 10 wt% PVA aqueous solution, is injected from the opposite side through the interstices between the square capillary and the collection capillary that is the tapered cylindrical capillary with a larger tip, as shown on the right of Figure 2a. We use $CaCl_2$ to increase the osmotic pressure of the continuous phase; it has essentially the same osmotic pressure as that of the core phase. The W/O/W double emulsion drops are formed at the tip of the injection capillary, as shown in Figure 2b and Movie S1 in the Supporting Information. Each double emulsion droplet consists of a middle oil layer inhomogeneously surrounding an inner aqueous core. After droplet generation, we crosslink the monomers in the middle oil phase in situ by exposing to UV light in the collection capillary to quickly form a solidified polymeric shell through a rapid thiol-ene reaction. As a result, the inhomogeneity in the microcapsule shell thickness can be fixed. The resultant microcapsules have an inhomogeneous shell thickness, as indicated by the red rings in Figure 2c. The shell thickness is characterized by obtaining scanning electron microscopy (SEM) images of the cross-sections of the microcapsules; an example is shown in Figure 2d. The thinnest part of shell is around 600 nm in thickness as shown in Figure 2d (inset) and the thickest portion of the shell is as large as 40 µm in thickness, confirming the inhomogeneity in the shell thickness.

To demonstrate the controllability of the inhomogeneous microcapsules, we change the flow rates of the middle phase $Q_m$ and the inner phase $Q_i$ to tune their ratio $Q_m/Q_i$, while keeping the ratio of their sum to the flow rate of outer phase constant. We find the geometries of the inhomogeneous microcapsules vary with the change of $Q_m/Q_i$, with a higher $Q_m/Q_i$ leading to a higher inhomogeneity of the shell, as shown in Figure 2e(i–iv). To quantitatively investigate the inhomogeneity of the microcapsules, we define the inhomogeneous microcapsule as having a geometry of outer radius $R$, inner radius $r$, average thickness $t$, and distance $\delta$ moved by inner water droplets, as illustrated in the inset in Figure 2f. The values of these parameters of inhomogeneous microcapsules prepared at different flow rate ratios are shown in Table S1 (Supporting Information). The shell inhomogeneity can be quantified by the ratio $\delta/t$.[28] We study the dependence of $\delta/t$ on $Q_m/Q_i$, confirming $\delta/t$ increases with increasing $Q_m/Q_i$, as shown in Figure 2f. This result indicates that we can control the inhomogeneity of microcapsules by simply tuning the flow rate ratio of the middle phase to the inner phase.

To probe the mechanical response of these inhomogeneous microcapsules, we prepare microcapsules containing a sucrose core with a high internal osmolarity, and subject the microcapsules to osmotic shock by adding a large amount of deionized (DI) water into the microcapsule suspensions. We use confocal microscopy to visualize the swelling and rupture of the microcapsules. Under hypotonic conditions, where the osmotic pressure of the inner core is higher than that of the external solution, the osmotic pressure difference across the shell

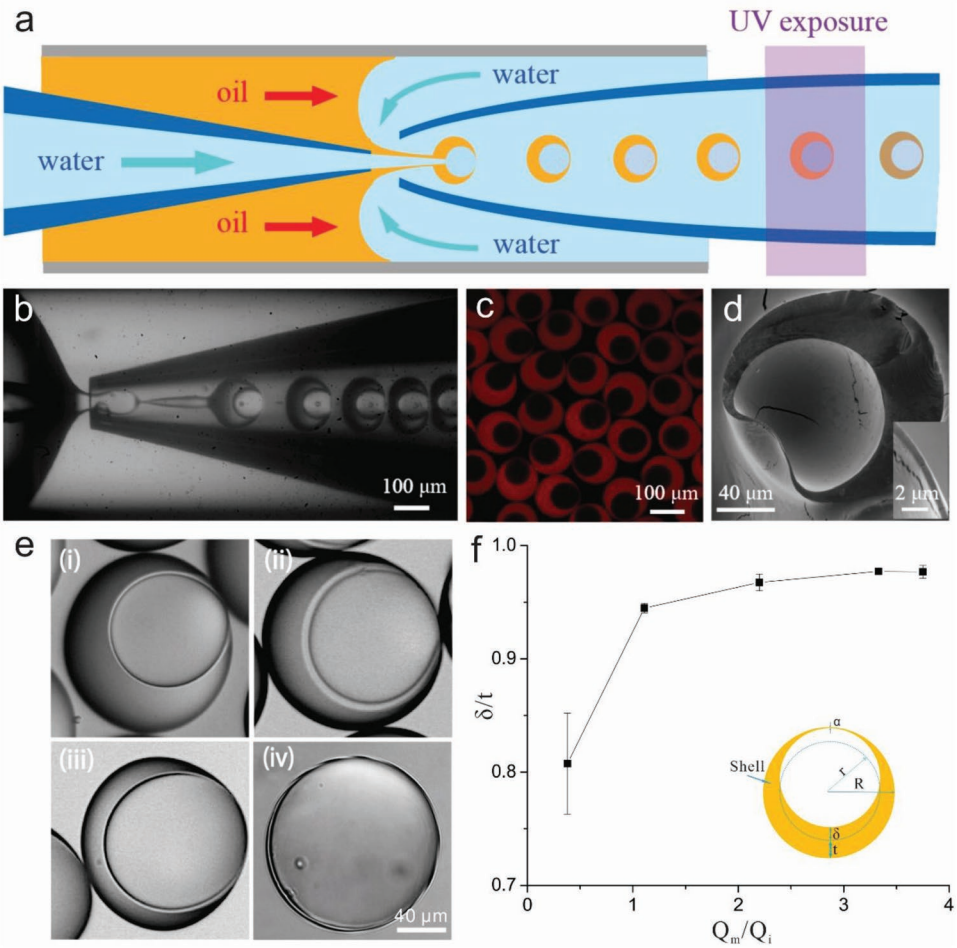


**Figure 2.** Microfluidic fabrication of inhomogeneous microcapsules. a) Schematic illustration of fabrication of inhomogeneous double emulsion droplets followed by UV exposure. b) Optical image of inhomogeneous double emulsion droplets formed in a glass capillary microfluidic device. c) Confocal image of inhomogeneous microcapsules with the shell labeled by Nile red. d) SEM image showing the cross-section of inhomogeneous microcapsule; inset shows the thinnest part. e) The microcapsules with different thickness inhomogeneity fabricated by varying flow rate ratio $Q_m/Q_i$: i) 3.33, ii) 2.20, iii) 1.11, iv) 0.38. Scale bar: 40 μm. f) Dependence of shell thickness inhomogeneity $\delta/t$ on $Q_m/Q_i$. Inset illustrates the microcapsule geometry.

causes water to diffuse into the microcapsules and makes them begin to swell at the thinnest part of shell. During the expansion, the deformation mainly localizes in this region, and the thickness of the polymeric shell membrane decreases, leading to an enhancement of the inward diffusion of water. Eventually, this part is unable to withstand deformation and mechanically cracks, as shown in **Figure 3**a and Movie S2 in the Supporting Information. After rupture, the opening is tens of micrometers in size, as seen in the SEM picture in Figure 3b. This is large enough for most encapsulated cargos, such as biomolecules or nanomaterials, to be released. While for the unruptured microcapsules, they are still intact to lock encapsulated cargos inside, as shown in Figure S1 (Supporting Information).

To systematically investigate the influence of shell inhomogeneity, $\delta/t$, on the fraction of microcapsules that burst, after adding DI water, we monitor an average of 150 microcapsules for each sample and calculate the rupture fraction as the ratio of the number of ruptured microcapsules to the total number of microcapsules. For each shell inhomogeneity, the fraction of burst microcapsules increases over time and eventually reaches a plateau, as shown in Figure 3c. We can see that with a larger inhomogeneity, the fraction of ruptured microcapsules increases faster with time and reaches a higher plateau. Thus, larger inhomogeneity results in more microcapsules rupture. By comparison, microcapsules with a nearly homogeneous, thin shell do not rupture when subjected to the same internal osmotic pressure; instead, they swell isotropically, ultimately reaching a volume that is increased by about 27 times, as shown in Figure S2 in the Supporting Information. This experiment demonstrates that the shell material itself is very tough, and can sustain the large level of mechanical strain; thus, an even higher osmotic pressure is required to make homogeneous microcapsules rupture. By contrast, microcapsules made of the same materials, but with an inhomogeneity of 0.97, achieve about 80% rupture fraction with the same osmotic pressure. This confirms that the inhomogeneous structure is crucial to make microcapsules rupture at a lower osmotic pressure.

We further study the effect of osmotic pressure, Π, on the rupture fraction. We prepare three sets of microcapsules with different amounts of shell inhomogeneity, and encapsulate

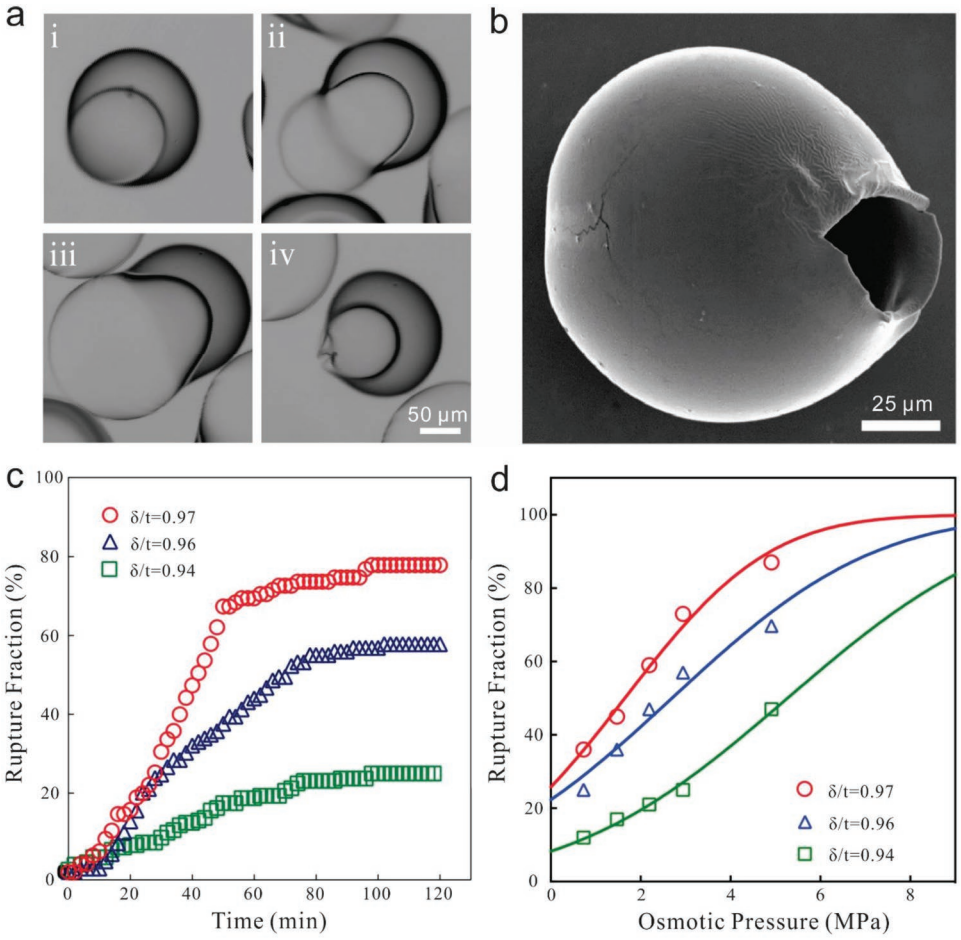


**Figure 3.** a) Optical images showing that shell swelling initiates at the thinnest part i–iii) and microcapsule ultimately ruptures iv); the microcapsules consist of aqueous core of 3 wt% PVA and 1.2 M sucrose with 2.94 MPa internal osmotic pressure and are dispersed in deionized water. b) SEM image showing the release orifice after capsule ruptures. c) Fraction of microcapsules ruptured over time, for three different shell thickness inhomogeneity, $\delta/t$. The internal osmotic pressure is 2.94 MPa. d) Fraction of microcapsules ruptured with different internal osmotic pressures, for three different shell thickness inhomogeneity, $\delta/t$.

sucrose solutions with five different concentrations in each set. We measure the fraction of ruptured capsules for each set, and find that increasing osmotic pressure increase the fraction of ruptured capsules, as shown in Figure 3d. Moreover, increasing inhomogeneity leads to increase in the fraction of ruptured capsules. The data can be described by a cumulative normal distribution function, as shown by the solid lines in Figure 3d. We extract two important parameters, the expectation, $\mu$, and the standard deviation, $\sigma$, of the normal distribution. We define the rupture osmotic pressure, $\Pi^* = \mu + 2\sigma$, and determine the dependence on shell inhomogeneity. Interestingly, we find a linear relationship between $\Pi^*$ and $\delta/t$, as shown in the Supporting Information; this provides an empirical relationship between $\delta/t$ and the rupture osmotic pressure, useful for design purpose.

To apply these inhomogeneous microcapsules as effective carriers for controlled release, we first test the impermeability of the inhomogeneous shell, which is an important parameter for long-term storage prior to triggered release. We encapsulate a fluorescent polymer fluorescein Isothiocyanate-dextran (FITC-Dextran) with a molecular weight of 3–5 kDa in the core and measure the change in the fluorescence intensity of the cores with elapsed time, using confocal microscopy. We find that the fluorescent polymer is completely retained after 30 d, as evidenced by the time-lapse fluorescent images in **Figure 4**a and fluorescence intensity profile in Figure 4b. The release kinetic of the encapsulated molecule is affected by the pore size of the capsule shell. As reported previously,[29] the thiol-ene photopolymerization allows us to fabricate capsules with highly impermeable shell that enables retention of small molecules in microcapsules. Considering the hydrodynamic radius of the FITC-Dextran is about 2 nm, which is much smaller than the size of most active biomolecules, such as antibodies, streptavidin, and enzymes, our result indicates that these microcapsules have a sufficiently impermeable shell that most of active biomolecules should be efficiently encapsulated.

As a demonstration of the application of these inhomogeneous microcapsules, we use protease as a model biological molecule. Protease can be found in all living organisms, from viruses to animals and humans, and it has great medical and pharmaceutical importance due to their key role in biological

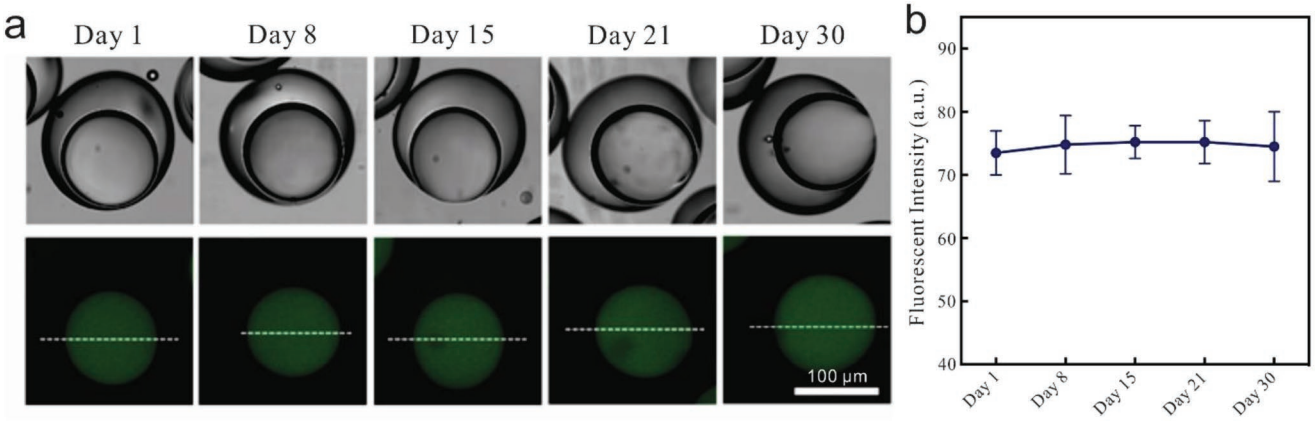


**Figure 4.** a) Optical and fluorescence images of microcapsules encapsulating FITC-dextran with molecular weight of 3–5 k. b) Fluorescent intensity profiles of the green fluorescence in microcapsules showing no obvious leakage up to 30 d after microcapsules were prepared.

processes and in the life-cycle of many pathogens.[30–32] We coencapsulate protease with sucrose in microcapsules with a nonuniform shell thickness. We incubate samples at 4 °C for up to 37 d, and then apply an osmotic shock to trigger the release of the encapsulated protease. We test its biological activity using the EnzChek Peptidase/Protease Assay Kit. The EnzChek peptidase/protease substrate comprises a fluorophore and a quencher moiety separated by an amino acid sequence. Upon sequence cleavage by protease, the fluorophore separates from the quencher and is free to emit a detectable fluorescent signal. The magnitude of the resultant signal is proportional to the degree of substrate cleavage, and can therefore be used to quantify the enzyme activity. We compare the activity of encapsulated protease to the same concentration of protease that has not been encapsulated. After 37 d incubation, the encapsulated protease retains over 91% of its initial activity, as shown in **Figure 5**. This result indicates the inhomogeneous microcapsules can effectively encapsulate biomolecules for long-term storage, and can be trigger-released by an applied osmotic shock.

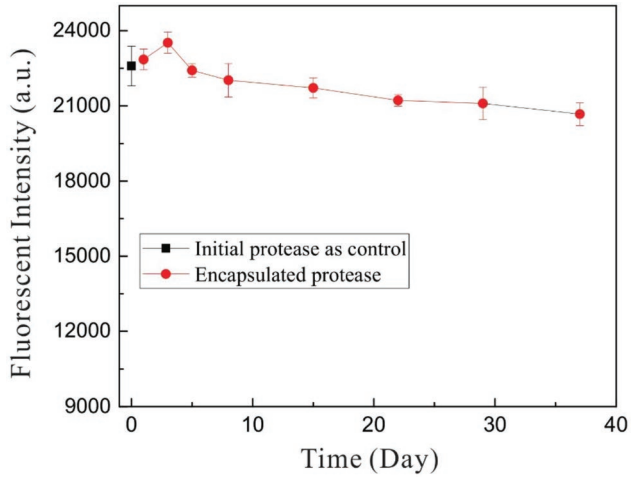


**Figure 5.** Enzymatic activity of protease as a function of incubation time in microcapsules.

In conclusion, we successfully demonstrate that inhomogeneous microcapsules are preferable for controlled release triggered by osmotic shock. A larger inhomogeneity leads to a larger fraction of ruptured capsules and the inhomogeneity of the microcapsules can be controlled by tuning the ratio of the flow rates of the middle and inner phases. By measuring the osmotic pressure dependence of the fraction of ruptured capsules, we define a rupture-osmotic-pressure and show that it exhibits a linear dependence on inhomogeneity; this enables us to predict the rupture behavior of microcapsules with a given inhomogeneity. Finally, inhomogeneous microcapsules can encapsulate biomolecules for long-term incubation and can be triggered by osmotic shock to release the encapsulated biomolecules without obviously impairing their biological activities. Our study provides a new approach to design effective carriers to encapsulate biomolecules and release them on-demand upon applying osmotic shock. Compared to other controlled release carriers, such as cells, nanoparticles, vesicles, or micelles,[33–37] our microcapsule system has high controllability, stability, and versatility. Therefore, it can be potentially applied in controlled release such as drug delivery.

## Experimental Section

*Chemicals*: The model biomolecule in this work was protease from Bacillus sp. (>16 U $g^{-1}$) purchased from Sigma-Aldrich. The polymers used were poly(ethylene glycol) divinyl ether (Mw 250, Sigma-Aldrich, USA), trimethylolpropane tris(3-mercaptopropionate) (Sigma-Aldrich, USA), PVA (Mw13000-23000, 87%–89% hydrolyzed, Sigma-Aldrich, USA), The photoinitiator used was 2,2-diethoxyacetophenone (Sigma-Aldrich, USA). Dichloromethane (DCM) (Sigma-Aldrich, USA) was used as organic solvent in the middle phase. Sucrose (BioXtra, Sigma-Aldrich, USA) and calcium chloride (Sigma-Aldrich, USA) were used to increase the osmotic pressure of inner and continuous phase, respectively. All reagents were used as received without further purification.

*Fabrication of Glass Capillary Device*: Glass capillary devices were used to fabricate microcapsules with inhomogeneous shell thickness. The injection and collection capillaries were prepared by tapering two glass cylindrical capillaries (Cat. No. 1B100-6; World Precision Instruments, Inc.), of inner and outer diameter 0.58 and 1.00 mm, respectively, to an inner diameter of 20 μm with a micropipetter puller (P-97, Sutter Instrument). These tapered glass capillaries were then polished to a final inner diameter of 80 and 160 μm with sand paper. The device

on a glass slide was assembled. Two glass capillaries were inserted into a square capillary (AIT Glass) with inner width of 1.05 mm from opposite direction. Prior to insertion, the cylindrical capillary with the smaller orifice was treated with n-octadecyltrimethoxyl silane to make the outer surface hydrophobic. The xy plane and z direction alignment of cylindrical capillaries nested in the square capillary was completed on a bright field microscope.

*Microcapsule Fabrication*: To form double-emulsion droplets, the three emulsion phases of W/O/W emulsion were injected into the glass capillaries using syringe pumps (Harvard Apparatus) and the production of double-emulsion droplets within the microfluidics device were recorded by an inverted microscope (Leica) equipped with a high-speed camera (Phantom V9). The syringe pumps were connected to the inlets of glass capillaries with plastic tubing of inner diameter 0.86 mm (Scientific Commodities Inc.). The photocurable monomers in the middle phase were polymerized in situ by UV exposure for 1–2 s in the collection capillary to form a solidified polymeric shell. Various formulations of inner phase consisting of 0.6, 1.2, and 2 M sucrose together with 3% PVA were used to fabricate the microcapsules. Sucrose was used to increase osmotic pressure. To avoid osmotic pressure, 0.2, 0.4, and 0.7 M $CaCl_2$ were added to 10% PVA solution as the outer phase. The flow rate of outer phase was maintained at value of 4500 µL $h^{-1}$. The inhomogeneities of shell thickness was tuned by varying the flow rate ratio of inner and middle phases. To maintain the size of capsules, the sum of flow rates of inner and middle phases constant was kept at a value of 1300 µL $h^{-1}$. Following the capsules fabrication, the capsules were washed with 0.5 M $CaCl_2$ solution five times to remove the organic solvent in the middle phase.

*Characterization*: To measure the microcapsule geometrical characteristics, either SEM or confocal microscopy was used. The middle fluid with red fluorescent dye was labeled, Nile red (Sigma-Aldrich) and confocal imaging was performed using a Leica TCS SP5 confocal laser scanning microscope, using a 10X dry objective. The SEM images of microcapsule cross-section were obtained on the ZEISS Ultra55 Field Emission Scanning Electron Microscope at an acceleration voltage of 4 kV after sputter-coating a Pt/Pd layer of 5 nm in thickness. The cross-section of a microcapsule was prepared by cutting liquid nitrogen frozen sample and then lyophilizing.

EnzCheck Peptidase/Protease Assay Kit (Invitrogen) was used to test the protease activities. A protease activity standard curve was prepared within 0–0.4 mU $mL^{-1}$ in triplicate, according to detection limit of 0.005 mU $mL^{-1}$. The encapsulated protease was released by applying osmotic shock and followed by brief sonication. The concentration of encapsulated protease was calculated according to the volume of inner phase and the total volume collected as well as the initial concentration of protease in inner phase. All released protease samples were diluted with Tri-HCl buffer (pH = 7.8) to the concentration within the range of the standard curve. The final volume in each microplate well was 100 µL with 50 µL of the released protease in Tri-HCl buffer and 50 µL of the substrate solution. After incubation at room temperature for 45 min, fluorescence intensity studies of the released protease were performed with a microplate fluorescence reader (excitation wavelength 502 nm and emission 530 nm).

## Supporting Information

Supporting Information is available from the Wiley Online Library or from the author.

## Acknowledgements

W.Z. and L.Q. contributed equally to this work. This work was supported by the National Science Foundation (DMR-1708729), the Harvard Materials Research Science and Engineering Center (DMR-1420570), and the Wyss Institute for Biologically Inspired Engineering at Harvard University.

## Conflict of Interest

The authors declare no conflict of interest.

## Keywords

biomolecules, controlled release, inhomogeneous microcapsules, microfluidics, osmotic pressure

Received: June 13, 2019
Revised: August 13, 2019
Published online:

[1] T. Kong, J. Wu, M. To, K. W. K. Yeung, H. C. Shum, L. Wang, *Biomicrofluidics* **2012**, *6*, 034104.
[2] P. T. d. Silva, L. L. M. Fries, C. R. d. Menezes, A. T. Holkem, C. L. Schwan, É. F. Wigmann, J. d. O. Bastos, C. d. B. d. Silva, *Ciência Rural* **2014**, *44*, 1304.
[3] V. Nedovic, A. Kalusevic, V. Manojlovic, S. Levic, B. Bugarski, *Procedia Food Sci.* **2011**, *1*, 1806.
[4] W. Zhang, A. Abbaspourrad, D. Chen, E. Campbell, H. Zhao, Y. Li, Q. Li, D. A. Weitz, *Adv. Funct. Mater.* **2017**, *27*, 1700975.
[5] X. Xie, W. Zhang, A. Abbaspourrad, J. Ahn, A. Bader, S. Bose, A. Vegas, J. Lin, J. Tao, T. Hang, H. Lee, N. Iverson, G. Bisker, L. Li, M. S. Strano, D. A. Weitz, D. G. Anderson, *Nano Lett.* **2017**, *17*, 2015.
[6] D.-H. Lee, M. Jang, J.-K. Park, *Biotechnol. J.* **2014**, *9*, 1233.
[7] T. M. S. Chang, *Science* **1964**, *146*, 524.
[8] S. S. Datta, A. Abbaspourrad, E. Amstad, J. Fan, S.-H. Kim, M. Romanowsky, H. C. Shum, B. Sun, A. S. Utada, M. Windbergs, S. Zhou, D. A. Weitz, *Adv. Mater.* **2014**, *26*, 2205.
[9] M. F. Bédard, B. G. De Geest, A. G. Skirtach, H. Möhwald, G. B. Sukhorukov, *Adv. Colloid Interface Sci.* **2010**, *158*, 2.
[10] X. Wang, J. Feng, Y. Bai, Q. Zhang, Y. Yin, *Chem. Rev.* **2016**, *116*, 10983.
[11] J. G. Werner, S. Nawar, A. A. Solovev, D. A. Weitz, *Macromolecules* **2018**, *51*, 5798.
[12] J. G. Werner, B. T. Deveney, S. Nawar, D. A. Weitz, *Adv. Funct. Mater.* **2018**, *28*, 1803385.
[13] F. Huang, W.-C. Liao, Y. S. Sohn, R. Nechushtai, C.-H. Lu, I. Willner, *J. Am. Chem. Soc.* **2016**, *138*, 8936.
[14] S.-H. Hu, S.-Y. Chen, D.-M. Liu, C.-S. Hsiao, *Adv. Mater.* **2008**, *20*, 2690.
[15] S. J. Leung, M. Romanowski, *Adv. Mater.* **2012**, *24*, 6380.
[16] H. Zhang, A. I. Cooper, *Adv. Mater.* **2007**, *19*, 2439.
[17] K. Liang, G. K. Such, Z. Zhu, Y. Yan, H. Lomas, F. Caruso, *Adv. Mater.* **2011**, *23*, H273.
[18] J. Liu, A. Debuigne, C. Detrembleur, C. Jérôme, *Adv. Healthcare Mater.* **2014**, *3*, 1941.
[19] P. D. Thornton, R. J. Mart, R. V. Ulijn, *Adv. Mater.* **2007**, *19*, 1252.
[20] L.-Y. Chu, T. Yamaguchi, S. Nakao, *Adv. Mater.* **2002**, *14*, 386.
[21] E. Loiseau, F. Niedermair, G. Albrecht, M. Frey, A. Hauser, P. A. Rühs, A. R. Studart, *Langmuir* **2017**, *33*, 2402.
[22] Y. Taguchi, R. Yamamoto, N. Saito, M. Tanaka, *J. Encapsulation Adsorpt. Sci.* **2014**, *4*, 15.
[23] B. C. Dave, K. Deshpande, M. S. Gebert, J. C. McAuliffe, *Adv. Mater.* **2006**, *18*, 2009.
[24] K. Y. Lee, M. C. Peters, D. J. Mooney, *Adv. Mater.* **2001**, *13*, 837.
[25] I. G. Nichols, *J. Natl. Dent. Assoc.* **1922**, *9*, 145.
[26] M. P. Goldman, J.-J. Guex, in *Sclerotherapy*, 6th ed. (Eds: M. P. Goldman, R. A. Weiss), Elsevier, Philadelphia, PA **2017**, p. 173.

[27] A. S. Utada, E. Lorenceau, D. R. Link, P. D. Kaplan, H. A. Stone, D. A. Weitz, *Science* **2005**, *308*, 537.
[28] S. S. Datta, S.-H. Kim, J. Paulose, A. Abbaspourrad, D. R. Nelson, D. A. Weitz, *Phys. Rev. Lett.* **2012**, *109*, 134302.
[29] D. V. Amato, H. Lee, J. G. Werner, D. A. Weitz, D. L. Patton, *ACS Appl. Mater. Interfaces* **2017**, *9*, 3288.
[30] J. A. Mótyán, F. Tóth, J. Tőzsér, *Biomolecules* **2013**, *3*, 923.
[31] D. F. Carmignac, *Cell Biochem. Funct.* **2003**, *21*, 298.
[32] C. López-Otín, J. S. Bond, *J. Biol. Chem.* **2008**, *283*, 30433.
[33] P. Zavala-Rivera, K. Channon, V. Nguyen, E. Sivaniah, D. Kabra, R. H. Friend, S. K. Nataraj, S. A. Al-Muhtaseb, A. Hexemer, M. E. Calvo, H. Miguez, *Nat. Mater.* **2012**, *11*, 53.
[34] M. E. Hartnett, C. M. Garcia, P. A. D'Amore, *Invest. Ophthalmol. Visual Sci.* **1999**, *40*, 2945.
[35] K. Olbrich, W. Rawicz, D. Needham, E. Evans, *Biophys. J.* **2000**, *79*, 321.
[36] M. Song, Y. Li, A. Ning, S. Fang, B. Cui, *J. Drug Delivery Sci. Technol.y* **2010**, *20*, 349.
[37] F. Arriagada, G. Günther, I. Zabala, J. Rubio-Retama, J. Morales, *AAPS PharmSciTech* **2019**, *20*, 202.